ELSEVIER

Chemical Engineering Journal 135 (2008) 71–77

Chemical Engineering Journal

www.elsevier.com/locate/cej

A pilot-scale continuous-jet hydrate reactor

Phillip Szymcek, Scott D. McCallum, Patricia Taboada-Serrano, Costas Tsouris *

Oak Ridge National Laboratory, P.O. Box 2008, Oak Ridge, TN 37831-6181, USA

Received 24 September 2006; received in revised form 14 March 2007; accepted 16 March 2007

Abstract

A three-phase, pilot-scale continuous-jet hydrate reactor (CJHR) has been developed for the production of gas hydrates. The reactor receives water and a hydrate-forming species to produce the solid gas hydrate. The CJHR has been tested for the production of CO_2 hydrate for the purpose of ocean carbon sequestration. Formation of CO_2 hydrate was investigated using various reactor/injector designs in a 72-l high-pressure vessel. Designs of the CJHR varied from single-capillary to multiple-capillary injectors that dispersed (1) liquid CO_2 into water or (2) water into liquid CO_2. The novel injector is designed to improve the dispersion of one reactant into the other and, thus, eliminate mass transfer barriers that negatively affect conversion. An additional goal was an increase in production rates of two orders of magnitude. The designed injectors were tested in both distilled and saline water. Hydrate production experiments were conducted at different CO_2 and water flow rates and for pressures and temperatures equivalent to intermediate ocean depths (1100–1700 m). The pilot-scale reactor with the novel injection system successfully increased hydrate production rates and efficiency.

Keywords: Gas hydrate reactor; Carbon dioxide hydrate; Ocean carbon sequestration

1. Introduction

Gas hydrates belong to a larger group of compounds known as clathrates. Clathrates are nonstoichiometric crystalline compounds that consist of hydrogen-bonded networks of water molecules and encased gas molecules, which stabilize the usually unstable empty clathrate structure through van der Waals forces. Gas hydrates are thermodynamically stable at high pressures and near the freezing temperature of pure water [1]. Although the specific conditions for temperature and pressure vary depending on the gas, most low-molecular-weight gases will form hydrates. Some common hydrate-forming gases include methane, nitrogen, carbon dioxide, hydrogen sulfide, and low-molecular-weight hydrocarbons.

Gas hydrates, which occur naturally, constitute an undesired product during gas production and gas transport operations. They are, however, being considered for various industrial applications. Methane hydrates occur naturally in sediments in the deep oceans and permafrost regions and constitute an extensive hydrocarbon reservoir [2]. Some of the potential industrial applications of gas hydrates include water desalination, gas separations, and energy storage and transportation. Carbon dioxide hydrates are currently of particular interest as a medium for marine sequestration of anthropogenic carbon dioxide [3].

Global atmospheric emissions of CO_2 are predicted to increase from 7.4 Gt carbon per year in 1997 to 26 Gt per year by 2100 [4]. Marine sequestration of CO_2, a possible means to counteract the increase in atmospheric CO_2, involves the injection of some form of CO_2 into the deep ocean. In general, infrastructure and implementation costs of carbon injection increase with injection depth, while residence times for sequestered CO_2 increase with increased injection depth [1]. Sequestering CO_2 as hydrate has potential advantages over most methods proposed for marine CO_2 sequestration. Because this technique requires a shallower depth of injection when compared with other ocean sequestration methods, the costs of CO_2 hydrate sequestration may be lower. The produced hydrate may also sink to greater depths, allowing for slow release of CO_2 to the environment and increasing the residence time of CO_2 in the ocean [5,6].

Previous studies have successfully used different continuous reactor designs to produce CO_2 hydrates in both laboratory and field settings [5–11]. Continuous hydrate formation was investigated by Currier et al. [10] for the purpose of flue-gas separation. In that work, hydrate was produced by mixing a continuous flow of cooled flue gas with water. Partial CO_2 separation from flue

---

* Corresponding author. Tel.: +1 865 241 3246; fax: +1 865 241 4829.
E-mail address: tsourisc@ornl.gov (C. Tsouris).

1385-8947/$ – see front matter © 2007 Elsevier B.V. All rights reserved.
doi:10.1016/j.cej.2007.03.029

gas was achieved at conditions approaching those required for industrial applications for the production of gas hydrate. Tajimi et al. [8] utilized a continuous-stirred-tank reactor for the production of gas hydrate, and a version of this reactor was later tested as an injection method for ocean CO_2 sequestration using simulated field conditions [9]. A laboratory-scale continuous-jet hydrate reactor (CJHR) was developed at Oak Ridge National Laboratory to produce gas hydrate [5,11]. This reactor was initially designed to produce CO_2 hydrate for marine carbon dioxide sequestration [11] and has been tested in the field to verify its effectiveness [6]. The pilot-scale CJHR described in this paper constitutes a scale-up design of the laboratory-scale CJHR presented by Tsouris et al. [6] and West et al. [11]. The scale-up process described in this paper constitutes an intermediate, but necessary, step between laboratory-scale production of hydrate and production of hydrate at a larger scale.

2. Pilot-scale CJHR

As previously indicated, the objective in developing the pilot-scale CJHR described in this work is marine carbon dioxide sequestration; and thus, results from this research involve primarily the application of the CJHR for this purpose. The main objective to be achieved via the scale-up process is to increase hydrate production rates while increasing reactant conversion.

The scaled-up CJHR consumed 0.80–3.00 l/min water (typically 2.00 and 3.00 l/min), and 0.33–0.66 l/min CO_2 (typically 0.66 l/min). On the other hand, the laboratory-scale CJHR consumed 15–25 ml/min water and 2–10 ml/min CO_2. Therefore, the increase in production rate of hydrate was approximately two orders of magnitude. During the scale-up process, the ratio of H_2O flow rate to CO_2 flow rate that was introduced to the reactor remained constant at the values determined via the laboratory-scale reactor, because those values are determined by the stoichiometry of hydrates. In the case of CO_2 hydrates, the estimated theoretical stoichiometry for hydrate formation corresponds to 5.75 mol of H_2O per mole of CO_2. Experiments were conducted with mol ratios in excess with respect to theoretical stoichiometry (from 7.5 to 23.1 mol of H_2O per mole of CO_2). Excess water increases mixing, and water will not be the limiting reactant in ocean sequestration applications.

Via its new injector designs, the pilot-scale CJHR was modified to overcome the product-limited aspects of hydrate production and, thus, to decrease the amounts of unconverted CO_2 and H_2O. The formation of CO_2 hydrate constitutes a product-limited reaction [12]. At favorable thermodynamic conditions, hydrate formation occurs instantaneously at the CO_2/H_2O interface at given temperatures and pressures, and a solid layer of CO_2 hydrate is formed over the entire surface area of the interface. Therefore, the potential for hydrate formation is limited by a surface barrier to mass transfer that prevents the interaction between the two reactants, thus diminishing reaction rates and limiting conversion. A means of reducing mass transfer resistance is to increase interfacial area. In addition to mass transfer limitations, the formation of hydrate releases heat, a process that may also slow further hydrate formation in the reactor.

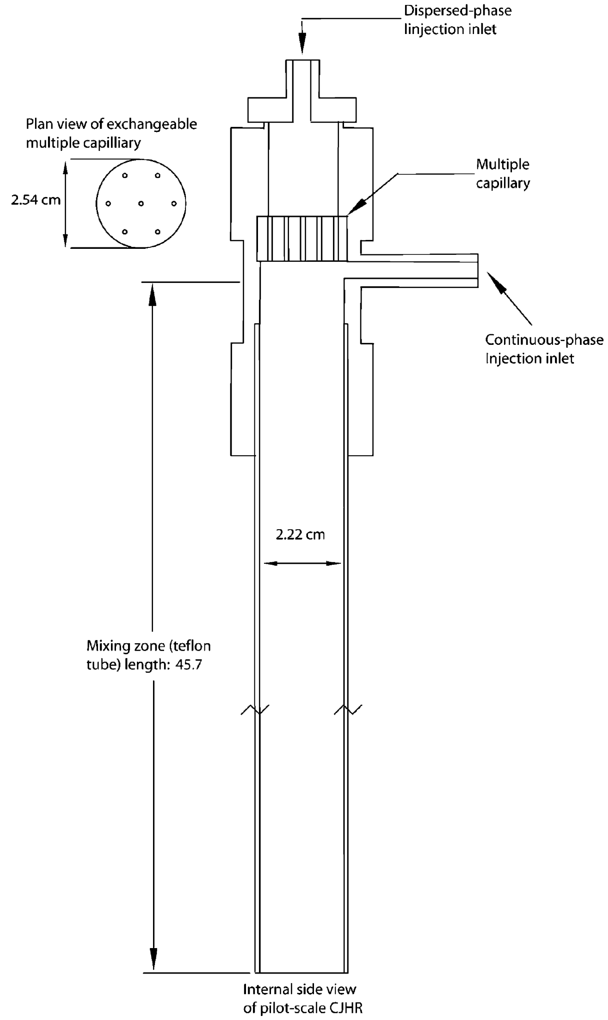

Fig. 1. Schematic of the continuous-jet hydrate reactor.

Maximizing the surface area of interaction between reactants during hydrate formation can be achieved by dispersing one of the hydrate-forming species into a continuous flow of the other hydrate-forming species, in this case CO_2 or H_2O. Ideally, the dispersed phase should be sprayed into the continuous phase using the smallest possible droplet size. Fig. 1 presents a schematic of the pilot-scale CJHR. The two reactants are introduced to the CJHR through different inlets. One of the reactants is forced through a capillary injector, in order to break the flow into small droplets.

To ensure that the reactor could work in a hydrodynamic jet break-up regime within a spray mode while maintaining high flow rates and low back-pressures, different capillary sizes and configuration designs were tested. Capillaries with diameters ranging from 0.397 to 3.175 mm were used in a single-capillary or seven multi-capillary arrays. The capillary diameters were selected to achieve spray regimes for specified production rates, as given by the Ohnesorge and Reynolds numbers [13]. In Fig. 2, all the points corresponding to different injector designs tested in the pilot-scale CJHR fall in the region of spray mode.

As a result of the decrease in droplet size, the production of hydrate in the spray regime was expected to result in high

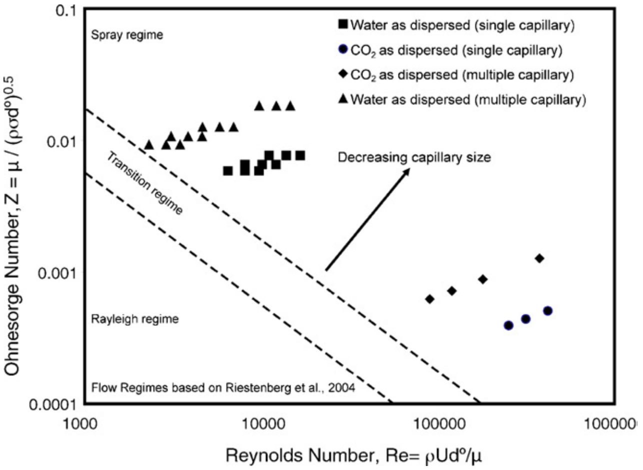

Fig. 2. Diagram of the jet breakup regimes achieved by the different injector designs tested in this work. Jet break-up regimes are identified by Ohnesorge and Reynolds numbers.

surface areas between the two phases containing the reactants. Therefore, larger conversions of CO_2 were expected to take place while the droplets traveled through the mixing zone. Additionally, the increase in the rate of formation of hydrate particles due to the reduction of mass transfer barriers was expected to allow for aggregation and consolidation of individual particles into larger masses of solid hydrate product.

3. Experimental methods

The pilot-scale CJHR allows for CO_2 to be either the continuous or the dispersed phase. Therefore, both scenarios were tested during this work—not only to determine which injector design was optimal for carbon sequestration applications in terms of capillary set up and dimensions but also to determine which arrangement would minimize the mass transfer limitations during hydrate production. Hydrate production was tested with either CO_2 or H_2O as the dispersed phase inside the reactor in experiments conducted using distilled water. Once the dispersed phase that lead to higher conversions was determined, tests were performed with saline water as well. Saline water was synthesized by using Instant Ocean® (Aquarium Systems, Mentor, OH) to a concentration of 35 ppt.

As shown in Fig. 1, the CJHR consists of a 13.3-cm headpiece with interchangeable inputs for hydrate-forming species and water and a 45.7-cm stainless steel tube. The dispersed-phase species flows through a single inlet on the top of the headpiece through an exchangeable capillary injector of 1.27-cm length and varying diameter (Fig. 1). The continuous-phase species flows into the reactor through an inlet directly below the exchangeable capillary injector. Hydrate product particles are produced in the mixing zone inside the stainless steel tube and are eventually extruded from the reactor.

The CJHR was mounted inside the Seafloor Process Simulator (SPS), a cylindrical Hastelloy C-22 vessel of 31.75-cm diameter, 91.44-cm length, and 72-l volume [14]. The vessel is equipped with several sapphire windows and sampling ports and can be maintained at pressures of up to 20 MPa. The SPS allows operational pressures equivalent to those encountered at various ocean depths to be maintained during laboratory experiments. The entire reactor was submerged and at equilibrium with the vessel. This set-up required the use of a submersible pump (Seabird SBE 5T) to circulate water, at a controlled rate, from within the SPS into the CJHR. Within the CJHR, the water was then mixed with liquid CO_2 injected from outside the SPS. This CO_2 was injected via a pulsed-flow pump from a pressurized cylinder. During the operation, water was recycled. The SPS was configured with a pressure transducer, and a thermocouple was submerged below the waterline within the simulator. LabView software was used to monitor and record internal pressure and temperature conditions. The SPS was filled with 60 l of distilled or saline water, and nitrogen was used to pressurize the vessel. The scale-up experiments were visually recorded with a Sony Firewire (XCD-X710CR) camera connected to a personal computer, which permitted the visual determination of degrees of consolidation and relative buoyancy of the hydrate product.

4. Results and discussion

In terms of CO_2 ocean carbon sequestration, the relative density of the CO_2 hydrate particles with respect to the surrounding water determines the success of injection operations. The density of the hydrate particles is determined by the conversion achieved during hydrate formation, and the degree of consolidation is determined by the degree of aggregation of individual, small hydrate particles in the mixing zone. Therefore, the performance of each capillary injector could be monitored in terms of the operating conditions required to produce consolidated, sinking hydrates. The performance of different injector designs are reported in terms of degree of consolidation and buoyancy of hydrate particles. In general, injector designs capable of producing consolidated sinking hydrates at lower pressures (i.e., shallower injection depths) at higher flow rates and ambient temperature conditions (i.e., typical ocean temperatures) are desirable.

The pilot-scale CJHR was used to successfully produce liquid $CO_2/H_2O/CO_2$-hydrate heterogeneous aggregates, an example of which is provided in Fig. 3. The aggregates presented different degrees of consolidation depending on which reactant was used as dispersed phase, on which injector design was tested, and on the conditions of operation selected. These factors also determined the relative density of the hydrate aggregates with respect to the surrounding water. For purposes of discussion, aggregates with open, fractal-like structures are labeled as unconsolidated (U), while solid-like aggregates that resemble products of an extrusion process are labeled as consolidated (C). In a similar way, the relative density of the hydrate produced was assessed visually via its buoyancy, with aggregates labeled as sinking (S), neutrally buoyant (NB), or floating (F).

Table 1 presents the performance of different injectors when using either H_2O or CO_2 as the dispersed phase. The performance is reported in terms of the minimum pressure required to obtain consolidated sinking hydrate-composite particles.

On the basis of the data in Table 1, CO_2 as dispersed phase proved to be more efficient in the conversion of CO_2 into hydrate.

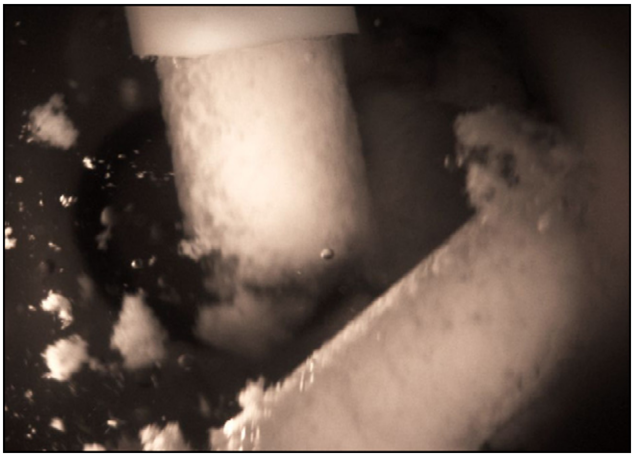

Fig. 3. Photograph of liquid CO_2/H_2O/CO_2-hydrate heterogeneous aggregates produced in the CJHR.

For example, with a 1.191-mm multiple-capillary injector, production of consolidated sinking hydrate aggregates from H_2O as dispersed phase required pressures over 13.1 MPa and temperatures lower than 2.5 °C. These parameters translate into greater injection depths and, thus, higher operation costs. On the other hand, the use of CO_2 as dispersed phase at similar flow rates (2.00 l/min of water and 0.66 l/min of CO_2) resulted in the formation of consolidated sinking hydrate at pressures as low as 6.9 MPa and ambient temperatures as high as 5 °C—a scenario that is economically more attractive. The difference in the performance between water and CO_2 as the dispersed phase can be explained by the expected increased droplet coalescence when water is used as the dispersed phase. At similar H_2O:CO_2 ratios, water as the dispersed phase will yield a higher ratio of droplet to continuous phase, because the flow rate is higher than that of liquid CO_2. The larger concentration of water droplets in the mixing zone results in coalescence, increasing the size of the water droplets and ultimately decreasing mass transfer rates and the proportion of CO_2 consumed by the reaction. Due to the stoichiometry of hydrate crystals, H_2O:CO_2 ratios during hydrate formation are always kept higher than 2, and, thus, the lower injection rates of CO_2 in all cases (1) result in less droplet coalescence in the mixing zone and (2) effectively maintain high surface areas. An additional factor contributing to the better performance of CO_2 as the dispersed phase may be the pulsed nature of the flow of CO_2 into the injector. On the basis of these findings, CO_2 was selected as the dispersed phase for further testing.

The data in Table 1 indicate that single-capillary injectors perform less efficiently than multiple-capillary injectors. This finding can be verified via a detailed comparison of the performance of a single-capillary injector and that of a multiple-capillary injector that have similar total cross-sectional areas at similar operational conditions. Table 2 summarizes the characteristics of hydrate product obtained with a 3.175-mm single-capillary injector and that obtained via a 1.191-mm multiple-capillary injector. The total cross-sectional areas of these single-capillary and multiple-capillary injectors are 7.913 and 7.795 mm^2, respectively. The operational conditions correspond to a pressure of 11.7 MPa, water flow rates between 2.00 and 3.00 l/min, CO_2 flow rates between 0.33 and 0.66 l/min, and temperatures between 3.0 and 5.1 °C. In all cases, the multiple-capillary configuration yielded well-consolidated negatively buoyant hydrates, while the single-capillary configuration yielded poorly consolidated positively buoyant hydrate product.

The better performance of multiple-capillary injectors over single-capillary injectors can be attributed to the fact that for comparable flow rates and cross-sectional areas, multiple-capillary injectors result in dispersions of smaller droplet sizes of one reactant into the other. Therefore, conversions are expected to be higher due to reduced mass transfer barriers during hydrate production. Additionally, the decreased diameters of multiple-capillary injectors that have total cross-sectional areas similar to those of single-capillary injectors allow for the utilization of comparably higher CO_2 flow rates while sustaining a spray-mode jet break-up regime. The smaller capillary diameters of multiple-capillary configurations yield higher Reynolds and Ohnesorge numbers, despite decreased flow rates per capillary, as depicted in Fig. 2, where data points corresponding to smaller capillary diameters move away from the transition regime.

Although working with multi-capillary injectors of the smallest possible diameter seems to constitute the best choice for production of hydrates, one has to consider that smaller capillary

Table 1

Minimum pressure required to produce consolidated sinking hydrate achieved via different injector designs

Injector design	Capillary diameter (mm)	Area of flow (mm^2)	Temperature (°C)	Minimum pressure for consolidated sinking hydrate $P_{\min}$ (MPa)
Water as dispersed phase				
Single capillary	3.969	12.3723	4.5	–[a]
Single capillary	3.175	7.9173	4.5	–[a]
Multiple capillary	1.588	13.8640	4.0	–[a]
Multiple capillary	1.191	7.7985	2.5	13.1
Carbon dioxide as dispersed phase				
Single capillary	3.175	7.9173	4.0	–[a]
Single capillary	2.381	4.4525	5.0	7.6
Multiple capillary	1.588	13.8640	3.3	7.6
Multiple capillary	1.191	7.7985	5.1	6.9
Multiple capillary	0.397	0.8665	4.2	6.2

[a] Sinking hydrate could not be obtained.

Table 2
Detailed comparison of the performance of a single-capillary injector and a multiple capillary injector with similar cross-sectional areas for dispersed phase flow

Operation conditions[a]			Single-capillary injector			Multiple-capillary injector		
P (MPa)	H_2O flow (l/min)	CO_2 flow (l/min)	Temperature (°C)	Diameter (mm)	Hydrate characteristics[b]	Temperature (°C)	Diameter (mm)	Hydrate characteristics[b]
11.7	2.00	0.33	4.0	3.175	C, NB	4.4	1.191	C, S
11.7	2.00	0.40	4.0	3.175	C, F	4.4	1.191	C, S
11.7	2.00	0.50	4.0	3.175	U, F	4.4	1.191	C, S
11.7	2.00	0.66	4.0	3.175	U, F	4.4	1.191	C, S
11.7	2.50	0.33	4.0	3.175	C, NB	4.4	1.191	U, S
11.7	2.50	0.40	4.2	3.175	C, NB	4.4	1.191	C, S
11.7	2.50	0.50	4.2	3.175	U, NB	4.4	1.191	C, S
11.7	2.50	0.66	4.2	3.175	U, F	4.4	1.191	C, S
11.7	3.00	0.33	4.2	3.175	C, NB	4.4	1.191	C, S
11.7	3.00	0.50	4.2	3.175	C, F	4.4	1.191	C, S
10.3	3.00	0.66	3.9	3.175	U, F	5.1	1.191	C, S

CO_2 was used as dispersed phase.

[a] P: pressure of operation.

[b] U: unconsolidated; C: consolidated; S: sinking; NB: neutrally buoyant; F: floating.

Table 3
Performance of the 1.191-mm multiple-capillary injector in distilled water

Pressure of operation (MPa)	CO_2 flow (l/min)	H_2O flow (l/min)	Temperature (°C)	Hydrate characteristics[a]
4.8	0.66	2	4.2	U, F
6.2	0.66	2	4.2	U, NB
6.7	0.66	2	4.1	C, S
7.6	0.66	2	4.1	C, S
11.7	0.66	2	4.4	C, S

[a] U: unconsolidated; C: consolidated; S: sinking; NB: neutrally buoyant; F: floating.

sizes may result in several operational drawbacks. Therefore, a compromise between obtaining parameters associated with desired conversion (e.g., consolidation degrees and relative buoyancy of hydrate particles) and operational constraints (e.g., high back-pressures and clogging problems) has to be achieved. Additionally, in the case of CO_2 as the dispersed phase with a multiple-capillary injector, Table 1 indicates that the minimum pressure necessary to obtain consolidated sinking hydrates increases marginally with decreasing capillary diameter size (e.g., from 6.2 MPa for a capillary with a diameter of 0.397 mm to 6.9 MPa for a capillary with a diameter of 1.191 mm). Another factor to consider when selecting a capillary size is that the presence of suspended material in seawater may result in more-pronounced operational problems with smaller-size capillary injectors. For all the reasons outlined above, the multiple-capillary injector with a capillary diameter of 1.191 mm was selected for further testing with distilled and saline water.

Table 3 summarizes the performance of the selected multiple-capillary injector in distilled water. Flow rates of 0.66 l/min and 2.0 l/min were used for CO_2 and H_2O, respectively, which is equivalent to an average molar ratio of 7.97 mol of H_2O per mole of CO_2. Consolidated sinking hydrate composites were produced in this reactor at pressures as low as 6.7 MPa and temperatures as high as 4.1 °C. Hydrate, though neutrally buoyant or floating, was still produced at pressures as low as 4.8 MPa. The characteristics of the hydrate product do not comply with the requirements for ocean sequestration purposes at very low pressures because floating or neutrally buoyant hydrate particles would dissociate at depths within the mixed layer in the oceans, allowing for CO_2 to be released into the atmosphere, and, thus, defeating the whole purpose of the application of gas hydrates as a means for carbon sequestration. However, the production of hydrate at these conditions (i.e., 4.8 MPa and 4.2 °C) could be useful for other applications.

Table 4 summarizes the performance of the selected multiple-capillary injector in saline water. The data indicate that high pressures and lower temperatures are required for the production of consolidated hydrate. The density of saline water

Table 4
Performance of the 1.191-mm multiple-capillary injector in saline water

Minimum pressure for consolidated hydrate (MPa)	CO_2 flow (l/min)	H_2O flow (l/min)	Temperature (°C)	Hydrate characteristics[a]
13.1	0.66	2.0	4.7	C, F
11.7	0.66	2.0	3.5	C, F
11.7	0.66	2.0	3.0	C, NB
11.7	0.66	2.0	2.0	C, S/NB
11.7	0.66	2.0	1.5	C, S/NB
11.7	0.66	3.0	1.6	C, S
13.1	0.66	3.0	1.9	C, S

[a] U: unconsolidated; C: consolidated; S: sinking; NB: neutrally buoyant; F: floating.

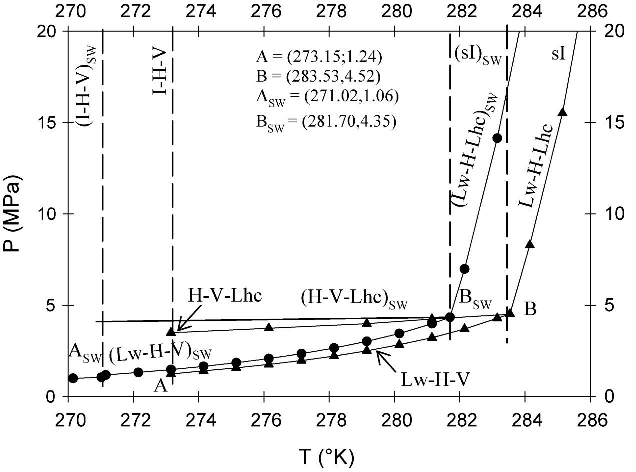

Fig. 4. Superposition of the CO_2-hydrate equilibrium diagrams for pure water (▲) and for seawater (●), where H, I, V, Lw and Lhc correspond to hydrate, ice, vapor, aqueous phase and liquid CO_2-rich phase, respectively. The letters A and B are used to identify quadruple points (i.e., points of coexistence of four phases), and sI indicates the type of hydrate structure (structure I). The subscript SW is used to distinguish the quadruple points, phases and hydrate structures related to the seawater equilibrium diagram.

(1.03–1.05 g/ml) is higher than that of distilled water. The density of CO_2 hydrate depends on the conversion achieved during formation, pressure, and temperature. For example, for conversions of 25%, the density of the produced CO_2 hydrate particles, which besides CO_2 hydrate, incorporate unconverted liquid CO_2 and seawater, overcomes the density of seawater only at pressures higher than 10 MPa [11]. Therefore, it was expected that achieving higher conversions would be necessary to produce consolidated sinking hydrate in saline water at comparable conditions of pressure and temperature to the ones in distilled water that result in consolidated, sinking hydrate.

The conversion achieved by the CJHR is a function not only of mixing conditions, but also of the driving force enabling hydrate formation. While no significant changes in mixing conditions are expected from the utilization of saline water instead of distilled water, appreciable changes are expected in terms of driving force. The driving force enabling hydrate formation constitutes the difference between operation conditions in the reactor and conditions of pressure and temperature at which hydrate equilibrium occurs [2]. The presence of salt in the system diminishes the activity of water and displaces the thermodynamically favorable conditions for hydrate formation toward higher pressures and lower temperatures [2]. For example, at 4 °C (277.15 K), the equilibrium pressure increases from 1.98 to 2.36 MPa, as seen in Fig. 4.

As indicated in Table 4, in addition to the constraints of temperature and pressures during the production of hydrates, consolidated sinking product can be obtained only by increasing the ratio of H_2O–CO_2 that is introduced to the CJHR. The presence of salt does not alter the stoichiometry of the reaction, and because H_2O constituted the continuous phase, increments in H_2O flow did not significantly alter the hydrodynamic conditions inside the reactor. The necessity for higher H_2O/CO_2 ratios may arise from the decreased activity of water, i.e., a decrease in the “effective” concentration of water available for hydrate formation.

During operation with seawater, the performance of the CJHR is limited by thermodynamic conditions. This limitation is removed if CO_2 injection occurs at greater depths, where the pressure is higher and the temperature is lower.

5. Conclusions

A pilot-scale CJHR was tested with injector designs that allowed for the increase in production rates of CO_2 hydrate while simultaneously increasing the efficiency of the process. Dispersing CO_2 in water within the spray regime enhanced process operations. A multiple-capillary injector with seven capillaries of 1.191-mm diameter, in a hexagonal array (with one capillary at the center) was selected as optimal in terms of carbon sequestration purposes in distilled water. This configuration also proved to be effective in saline water, although its efficiency in these conditions is bound by thermodynamic constraints.

The multiple-capillary injector design tested in the present work will be employed during operations involving deep ocean injections.

Acknowledgments

Gratefully acknowledged is support by the Ocean Carbon Sequestration Program, Office of Biological and Environmental Research, U.S. Department of Energy under Contract No. DE-AC05-00OR22725 with UT-Battelle, LLC. The authors are thankful to Dr. Tommy Phelps for stimulating discussions and helpful comments, and to Dr. M.K. Savage for editing the manuscript.

References

[1] J.H. van der Waals, J.C. Platteeuw, Clathrate solutions, Adv. Phys. Chem. 2 (1959) 1–57.

[2] E.D. Sloan Jr., Clathrate Hydrates of Natural Gases, 2nd ed., Marcel Dekker, New York, 1998.

[3] P. Brewer, G. Friederich, E.T. Peltzer, F. Orr, Direct experiments on the ocean disposal of fossil fuel CO_2, Science 284 (1999) 943–945.

[4] U.S. Department of Energy, Carbon Sequestration Research and Development; Office of Science and Office of Fossil Energy, U.S. Department of Energy, Washington DC, 1999.

[5] S.Y. Lee, L. Liang, D. Riestenberg, O. West, C. Tsouris, E. Adams, CO_2 hydrate composite for ocean carbon sequestration, Environ. Sci. Technol. 37 (2003) 3701–3708.

[6] C. Tsouris, C.P. Brewer, E. Peltzer, P. Waltz, D. Riestenberg, L. Liang, Hydrate composite particles for ocean sequestration: field verification, Environ. Sci. Technol. 38 (2004) 1499–1509.

[7] D. Riestenberg, C. Tsouris, P. Brewer, E. Peltzer, P. Walz, A. Chow, E.E. Adams, Field studies on the formation of sinking CO_2 particles for ocean carbon sequestration: effects of injector geometry on particle density and dissolution rate and model simulation of plume behavior, Environ. Sci. Technol. 39 (2005) 7287–7293.

[8] H. Tajima, A. Yamasaki, F. Kiyono, Continuous formation of CO_2 hydrate via a kinetics-type static mixer, Energy Fuels 18 (5) (2004) 1451–1456.

[9] H. Tajima, Y. Akihiro, F. Kiyono, Process design of a new injection method of liquid CO_2 at the intermediate depths in the ocean using a static mixer, Fuel Process Technol. 86 (2005) 1667–1678.

[10] R. Currier, D. Yang, L. Le, R. Martinez, M. Sedillo, S. Obrey, S. Tam, T. Lee, D. Spence, CO_2 hydrate formation in a continuous flow reactor, in: Proceedings of the Fifth Annual Conference on Carbon Capture & Sequestration, 2006, Paper 120.

[11] O.R. West, C. Tsouris, S. Lee, S. McCallum, Negatively bouyant CO_2–hydrate composite for ocean carbon sequestration, AIChE J. 29 (2003) 276–285.

[12] Y. Shindo, K. Sakaki, Y. Fujioka, H. Komiyama, Kinetics of the formation of CO_2 hydrate on the surface of liquid CO_2 droplet in water, Energy Convers. Manage. 37 (1996) 485–489.

[13] D. Riestenberg, E. Chiu, M. Gborigi, L. Liang, O.R. West, C. Tsouris, Investigation of jet breakup and droplet size distribution of liquid CO_2 and water systems—implications for CO_2 hydrate formation for ocean carbon sequestration, Am. Mineral. 89 (2004) 1240–1246.

[14] T.J. Phelps, J. Peters, O.R. Marshall, L. West, J.G. Blencoe, V. Alexiades, G.K. Jacobs, A new experimental facility for investigating the formation and properties of gas hydrates under simulated seafloor conditions, Rev. Sci. Instrum. 72 (2001) 1514–1521.